Cardiovascular pharmacology

Efficacy of selective NCX inhibition by ORM-10103 during simulated ischemia/reperfusion

Anita Kormos [a], Norbert Nagy [c], Károly Acsai [c], Krisztina Váczi [b], Szabina Ágoston [a], Piero Pollesello [d], Jouko Levijoki [d], Norbert Szentandrássy [b], Julius Gy. Papp [c], András Varró [a,c], András Tóth [a,c,*]

[a] Department of Pharmacology & Pharmacotherapy, University of Szeged, Dóm tér 12., 6722 Szeged, Hungary
[b] Department of Physiology, University of Debrecen, Debrecen, Hungary
[c] MTA-SZTE Research Group of Cardiovascular Pharmacology, Hungarian Academy of Sciences, Szeged, Hungary
[d] Orion Pharma, Espoo, Finland

ABSTRACT

In this study we evaluated the effects of selective Na^+/Ca^{2+} exchanger (NCX) inhibition by ORM-10103 on the $[Ca^{2+}]_i$ transient (CaT), action potential (AP), and cell viability in isolated canine ventricular cardiomyocytes exposed to a simulated ischemia/reperfusion protocol performed either alone (modeling moderate low-flow ischemia) or with simultaneous strophantidine challenge (modeling more severe low-flow ischemia). CaTs were monitored using a Ca^{2+}-sensitive fluorescent dye, APs were recorded by intracellular microelectrodes, and anaerobic shifts in cellular metabolism were verified via monitoring native NADH fluorescence. *Simulated ischemia* increased the NADH fluorescence, reduced the amplitudes of the AP and CaT and induced membrane depolarization. APs moderately shortened, CaTs prolonged. Diastolic $[Ca^{2+}]_i$ ($[Ca^{2+}]_{iD}$) level increased significantly during ischemia and further elevated following strophantidine application. *Reperfusion* normalized the NADH level, the amplitude of the AP and duration of the $[Ca^{2+}]_i$ transient, but only partially restored action potential triangulation and the amplitude of the CaT. $[Ca^{2+}]_{iD}$ decreased in untreated, but further increased in strophantidine-treated cells. 10 μM ORM-10103 significantly reduced the ischemic $[Ca^{2+}]_i$ raise in both untreated and strophantidine-treated cells. During reperfusion ORM-10103 decreased $[Ca^{2+}]_i$ and eliminated its diastolic elevation in untreated and strophantidine-treated cardiomyocytes. Following the application of ORM-10103 the detrimental effect of ischemia/reperfusion on cell viability and the reperfusion-induced increase in AP and CaT variabilities were substantially reduced, but ischemia-induced shifts in AP morphology were barely influenced. In conclusion, selective NCX inhibition by ORM-10103 is highly effective against ischemia/reperfusion induced pathologic alterations in $[Ca^{2+}]_i$ homeostasis, however, it fails to normalize untoward arrhythmogenic changes in AP morphology.

© 2014 Elsevier B.V. All rights reserved.

1. Introduction

Cardiac Na^+/Ca^{2+} exchanger has a pivotal role in removal of the excess Ca^{2+} (forward transport mode) entering mainly via L-type Ca^{2+} channels during the AP, however it may also contribute to Ca^{2+} entry (reverse transport mode). Therefore, its balanced activity is essential in maintaining cardiac $[Ca^{2+}]_i$ homeostasis and any abnormal change in its transport activity may severely impair the contractile function and the electrical activity of the beating heart.

During hypoxia the raise in $[Na^+]_i$ shifts the NCX into its reverse transport mode. The reduction in $[K^+]_i$ depolarizes the sarcolemma (Baczko et al., 2003; Tanaka et al., 2002), further facilitating reverse mode NCX activity and leads to gradual $[Ca^{2+}]_i$ accumulation. During the early phase of ischemia the major source of the $[Ca^{2+}]_i$ increase is the leaky SR (Zucchi and Ronca-Testoni, 1997), while during the late phase, $[Ca^{2+}]_i$ accumulation via NCX is accelerated (Bourdillon and Poole-Wilson, 1981; Haigney et al., 1992). During reperfusion the secondary $[Na^+]_i$ raise further activates the already high reverse mode transport, generating $[Ca^{2+}]_i$ overload and subsequently increased SR Ca^{2+} content. These alterations often lead to abnormal membrane potential changes (Volders et al., 2000) enhanced probability of diastolic Ca^{2+} releases (Diaz et al., 1997), enhanced arrhythmia propensity (early and delayed afterdepolarizations) and cellular injury

* Corresponding author at: Department of Pharmacology & Pharmacotherapy, University of Szeged, 6722 Szeged, Dóm tér 12. Hungary. Tel.: +360662 545 682; fax: +360662 545 680.
E-mail address: toth.andras@med.u-szeged.hu (A. Tóth).

(Talukder et al., 2009). During incomplete (low-flow) ischemia/reperfusion the changes in $[Na^+]_i$ and $[Ca^{2+}]_i$ homeostasis are less dramatic (Wei et al., 2007).

Up to present benzyloxyphenyl derivatives KB-R7943 and SEA0400 were considered as the best NCX inhibitors. In isolated rat cardiomyocytes exposed to simulated ischemia KB-R7943 reduced the $[Ca^{2+}]_i$ overload and delayed the onset of the contracture (Ladilov et al., 1999). The raise in $[Ca^{2+}]_i$ induced by the removal of extracellular Na^+, was blocked by 90% in the presence of KB-R7943 (Tokuno et al., 2000). In reoxygenated rat cardiomyocytes hypercontracture and $[Ca^{2+}]_i$ oscillations were significantly reduced in the presence of KB-R7943 (Schafer et al., 2001). Both SEA0400 and KB-R7943 inhibited the Na^+-dependent Ca^{2+} uptake in rat cardiomyocytes. Similar, positive effects of NCX inhibition were reported from isolated guinea pig papillary muscles and rat hearts (Anderson, 2002; Schafer et al., 2001; Wang et al., 2007). NCX inhibitors were shown to attenuate myocardial reperfusion injury using *in vivo* experimental models (Takahashi et al., 2003). Under normal conditions or during ischemia 1 μM SEA0400 had no apparent effect on AP configuration, but improved the recovery of action potentials after reperfusion (Acsai et al., 2007).

Previous data (Inserte et al., 2002; MacDonald and Howlett, 2008; Wei et al., 2007) suggest that inhibition of the reverse mode NCX activity during ischemia/reperfusion exert effective cardioprotection by reducing $[Ca^{2+}]_i$ overload and improving myocardial recovery during reperfusion. However, the inhibitors used in these studies were not fully selective (Birinyi et al., 2005), consequently the overall effect of NCX inhibition could not be quantitatively analyzed. Therefore, the aim of the present study was to evaluate the cardioprotective effect of a novel, selective NCX inhibitor, ORM-10103 (Jost et al., 2013) in isolated canine ventricular cardiomyocytes in conditions of simulated ischemia/reperfusion. This aim was accomplished by analyzing the *primary,* simulated ischemia/reperfusion induced shifts in characteristic variables on the CaT and AP and evaluating the *modulatory* effects of *selective, partial* NCX inhibition on these shifts. Supplementary experiments were also performed in order to directly *estimate and compare* the survival rate during ischemia and reperfusion of untreated and ORM-10103 treated cardiomyocytes.

2. Materials and methods

All animal experiments were carried out in compliance with the Guide for the Care and Use of Laboratory Animals (USA NIH Publication no. 86-23, revised 1996) and conformed to Directive 2010/63/EU of the European Parliament. Furthermore, all experimental protocols were approved by the Ethical Committee for Protection of Animals in Research of the University of Szeged, Hungary (Permit no. I-74-9/2009).

2.1. Isolation of canine left ventricular cardiomyocytes

Canine ventricular cardiomyocytes were isolated from adult mongrel dogs of either sex weighing 10 to 20 kg. Following sedation (xylazine, 1 mg/kg, i.v.) the animals were anaesthetized with 30 mg/kg thiopental and anticoagulated with sodium-heparin. The proper depth of anesthesia was carefully tested with pupilla and pain reflexes. Following right lateral thoracotomy the heart was quickly removed and immediately rinsed in oxygenated modified Locke's solution containing (in mM): Na^+ 140, K^+ 4, Ca^{2+} 1.0, Mg^{2+} 1, $Cl-$ 126, HCO_3- 25 and glucose 11. The pH of the solution, bubbled with 95% O_2 and 5% CO_2 at 37 °C, ranged from 7.35 to 7.45. Excised left ventricular segments were perfused at 37 °C through the anterior descending coronary artery using a gravity flow Langendorff apparatus. First, to remove the blood

the heart was washed for 5 min with isolation solution containing 1 mM Ca^{2+}, then the perfusate was switched to a Ca^{2+}-free solution containing (in mM) 135 NaCl, 4.7 KCl, 1.2 KH_2PO_4, 1.2 $MgSO_4$, 10 HEPES, 10 glucose, 20 taurine, 4.4 $NaHCO_3$, and 5 Na-Pyruvate (pH 7.2 with NaOH). 10 min later, 75 μM $CaCl_2$ and 150 U/ml collagenase (Worthington Type II), and 15 min later 0.35 U/ml protease (Sigma Type XIV) was added to the perfusate. Cell dissociation lasted for 30–40 min. At the end of this isolation process the tissue was minced and gently agitated. The myocytes were harvested and stored in the isolation solution containing 1 mM Ca^{2+} at room temperature for the same day or at 4 °C for next day recordings. Following restoration of the external $[Ca^{2+}]$ at least 60% of the cardiomyocytes were rod-shaped showing clear striation. During measurements the cells were perfused with Tyrode solution. The Tyrode solution contained (in mM): 144 NaCl, 0.4 NaH_2PO_4, 4 KCl, 0.53 $MgSO_4$, 1.8 $CaCl_2$, 5.5 glucose and 5 HEPES. The pH was set to 7.4 with NaOH. All measurements were performed at 37 °C.

2.2. Determination of cell viability

Freshly isolated, unloaded cardiomyocytes, subjected to the ischemia/reperfusion protocol were visually assessed, classified and counted in randomly selected microscopic fields (Olympus IX 71 inverted fluorescence microscope; 20 × objective). A representative, circular region of the microscopic field (region of interest; ROI), containing predominantly contracting cells, was used for analysis. Still images of the ROI were periodically captured by an Olympus digital photo camera (C-7070). In order to safely distinguish living and dead cells, instead of using vital dyes, we followed another, similarly effective classification, utilizing characteristic morphological variables, i.e. the shape and visibility of striation of the cells (Maddaford et al., 1999). Cardiomyocytes in the ROI were divided into two classes: **Class A:** cells with normal (not significantly shortened) shape, intact border and visible striation; **Class B:** cells dead or at the verge of death, in severe contracture, parallel striation cannot be observed. The cells were stimulated (1 Hz) throughout the experiment. The number of surviving and dead cells was determined several times (at 0th,1.5th,3rd, 4rth,10th,15th,23rd,24rth,26th,30th,32nd min) during the ischemia/reperfusion protocol.

2.3. Validation of the level of simulated ischemia via NADH measurements

Parallel to the shift from aerobic to anaerobic metabolism a substantial fraction of the intramitochondrial NAD^+ content is gradually reduced. Since only the reduced form, NADH is fluorescent, a raise in $[NADH]_m$ is considered as a direct indicator of ischemia. In this set of experiments NADH was excited at 360 nm, while the native cellular fluorescence was monitored at 450 nm. The relative magnitude of the momentary fluorescent shift compared to the maximal raise achieved following the application of 10 mM NaCN has been used to characterize the level of ischemia. Therefore, cardiomyocytes were stimulated at 1 Hz and the simulated ischemia/reperfusion protocol (i.e. 3–5 min normoxic control, 20 min simulated ischemia and 10 min reperfusion – see details below) was used. At the end of the protocol the cells were exposed to 10 mM cyanide, which quickly induced maximal NAD^+ reduction.

2.4. Monitoring $[Ca^{2+}]_i$ transients in single ventricular cardiomyocytes

$[Ca^{2+}]_i$ transients were monitored using a Ca^{2+}-sensitive fluorescent dye, Fluo 4. Isolated cardiomyocytes were loaded with

6 μM Fluo 4-AM (AM is the *membrane permeable* acetoxymethyl ester conjugated form of the dye) for 15 min at room temperature in dark. Loaded cells were mounted in a low volume imaging chamber (RC47FSLP, Warner Instruments) and field-stimulated at a rate of 1 Hz, while continuously superfused with normal (during control and reperfusion periods) or "simulated ischemic" Tyrode solution. Fluorescence measurements were performed on the stage of an Olympus IX 71 inverted fluorescence microscope. The dye was excited at 480 nm and the emitted fluorescence was detected at 535 nm. Optical signals were sampled at 1 kHz and recorded by a photon counting photomultiplier module (Hamamatsu, model H7828). Data acquisition and analysis were performed using a CAIRN Optoscan System. Alterations in $[Ca^{2+}]_i$ were characterized by the corresponding changes in background corrected fluorescence normalized to the control state (F/F_0). Amplitudes of the $[Ca^{2+}]_i$ transients were calculated as differences between systolic and diastolic values. Diastolic $[Ca^{2+}]_i$ levels were determined immediately before the onset of the stimulus. Systolic $[Ca^{2+}]_i$ was determined at the peak of the corresponding transient. $[Ca^{2+}]_i$ changes were expressed as fluorescence measured over basal unstimulated fluorescence (F/F_0). Background fluorescence levels were recorded for a few times during each experiment and were used to correct raw fluorescence data.

2.5. Recording of single cell action potentials

Single cell APs were recorded using conventional sharp microelectrodes. Selected cardiomyocytes were impaled with high-resistance (20–40 MΩ) electrodes filled with 3 M KCl. APs were recorded with an Axoclamp 900 A amplifier (Axon Instruments) and were analyzed using the Clampfit 10.0 software (Molecular Devices Corporation). Action potential parameters, such as amplitude, plateau level, duration (both APD_{25} and APD_{90}) and triangulation (APD_{90}–APD_{25}) of the AP, and the resting membrane potential were determined.

2.6. Introducing simulated ischemia

As in similar studies, simulated ischemia was introduced using a low pH, low pO_2, high K^+, glucose free, high lactate perfusion solution (composition (in mM): 123 NaCl, 6 NaHCO₃, 0.9 NaH₂PO₄, 8 KCl, 0.5 MgSO₄, 2.5 CaCl₂ and 20 lactate) (Louch et al., 2002). The cells were first perfused with normal Tyrode solution (*normoxia:* 3 min), then with simulated ischemic solution (*ischemia:* 20 min), and finally again with normal Tyrode solution (*reperfusion:* 10 min). During the ischemic period an oxygen-free gas combination (95% N_2+5% CO_2) was layered over the solution. Each cell was exposed to the ischemia/reperfusion cycle only once. The oxygen level in the ischemic solution was decreased to a very low level by heavily gassing the solution with the anoxic gas mixture. The pO_2 level in the solution was periodically checked using a clinical blood gas analyzer (Radiometer ABL 505). The pO_2 level was approximately 180 mmHg in normal Tyrode. This rapidly declined to about 32 mmHg (determined in the chamber) in the ischemic solution, which represents a reasonably high level of hypoxia.

2.7. Experimental protocols

In the present study 4 principal sets of experiments were performed: cell viability measurements, NADH measurements, $[Ca^{2+}]_i$ transient measurements and AP measurements. In order to reach maximal, but still selective inhibition of the exchanger, ORM-10103 has been used in 10 μM dose. At this dose no apparent effect of the inhibitor on further ion transporters (except a small inhibition of I_{Kr}) could be observed (Jost et al., 2013).

1) *Viability measurements:* Two subsets of experiments were performed. The ischemia/reperfusion protocols were identical to the corresponding subsets of the AP measurements (native, untreated and ORM-10103 treated cardiomyocytes). Since under normoxic conditions cell survival was usually close to 100% for at least an hour, no separate time control (TC) measurements were performed.
2) *NADH measurements:* Since NADH is inherently fluorescent, no cells in this group had to be loaded with external dye. Cardiomyocytes in the first subgroup were utilized as time control and were superfused with oxygenated Tyrode solution throughout the experiment; no simulated ischemia was introduced. The second subgroup of cells was subjected to a full cycle of ischemia/reperfusion (see above).
3) *$[Ca^{2+}]_i$ transient measurements:* These measurements were performed in cardiomyocytes loaded with Fluo 4-AM. Five subsets of experiments were performed. The first subset was used for *time control*; no ischemia/reperfusion (I/R) cycle was applied. In the second one (*untreated)* cells were subjected to a full cycle of ischemia/reperfusion. In the third one (*ORM-10103*) cells were pretreated with 10 μM of ORM-10103, the selective NCX inhibitor, at the end of the control period but prior to the ischemia/reperfusion cycle. The fourth and fifth subsets were similar to the second and third ones, with the exception that in order to substantially increase the driving force for reverse mode NCX activity these solutions also contained the Na^+/K^+-ATP-ase (NKA) inhibitor strophantidine (1 μM).
4) *AP measurements:* Three subsets of experiments were performed. The protocols were identical to the corresponding subsets of the $[Ca^{2+}]_i$ transient measurements (*i.e.* untreated, ORM-10103 treated and time control), but these measurements were performed using unloaded cardiomyocytes.

2.8. Variabilities of APD_{90}, APD_{25} and the $[Ca^{2+}]_i$ transient

The beat-to-beat variability of APD_{90}, APD_{25}, and CaT amplitude were calculated by the analysis of 50 consecutive action potentials or $[Ca^{2+}]_i$ transients from the steady-state section of the experiment, via using the following formulas:

$$BVR_{(ADP90)} = \Sigma(APD_{90}; i+1 - APD_{90}; i)/(n_{beats} x \sqrt{2})$$

$$BVR_{(ADP25)} = \Sigma(APD_{25}; i+1 - APD_{25}; i)/(n_{beats} x \sqrt{2})$$

Since the uncorrected CaT amplitude largely depends on non-specific variables (cell size, dye concentration and leakage) and this dependence would also be reflected in the variabilities, the simple formula used to calculate short term APD variabilities may not be suitable to properly characterize CaT variabilities. Therefore, we normalized the raw variability data to the mean CaT amplitude (CaT_{TC}), calculated from the corresponding time control experiments, as follows:

$$BVR_{(CaT)} = \Sigma(CaT \text{ amplitude}; i+1 - CaT \text{ amplitude}; i)/((n_{beats} x \sqrt{2}) \times \text{mean } CaT_{TC} \text{amplitude})$$

2.9. Materials

All materials were purchased from Sigma (St. Louis, Mo, USA) except for Fluo 4-AM (Life Technologies). ORM-10103 was a gift from Orion Pharma (Espoo, Finland).

2.10. Data processing and statistics

Individual cardiomyocytes—even if selected from the same isolation—show great variability in size and volume. Consequently,
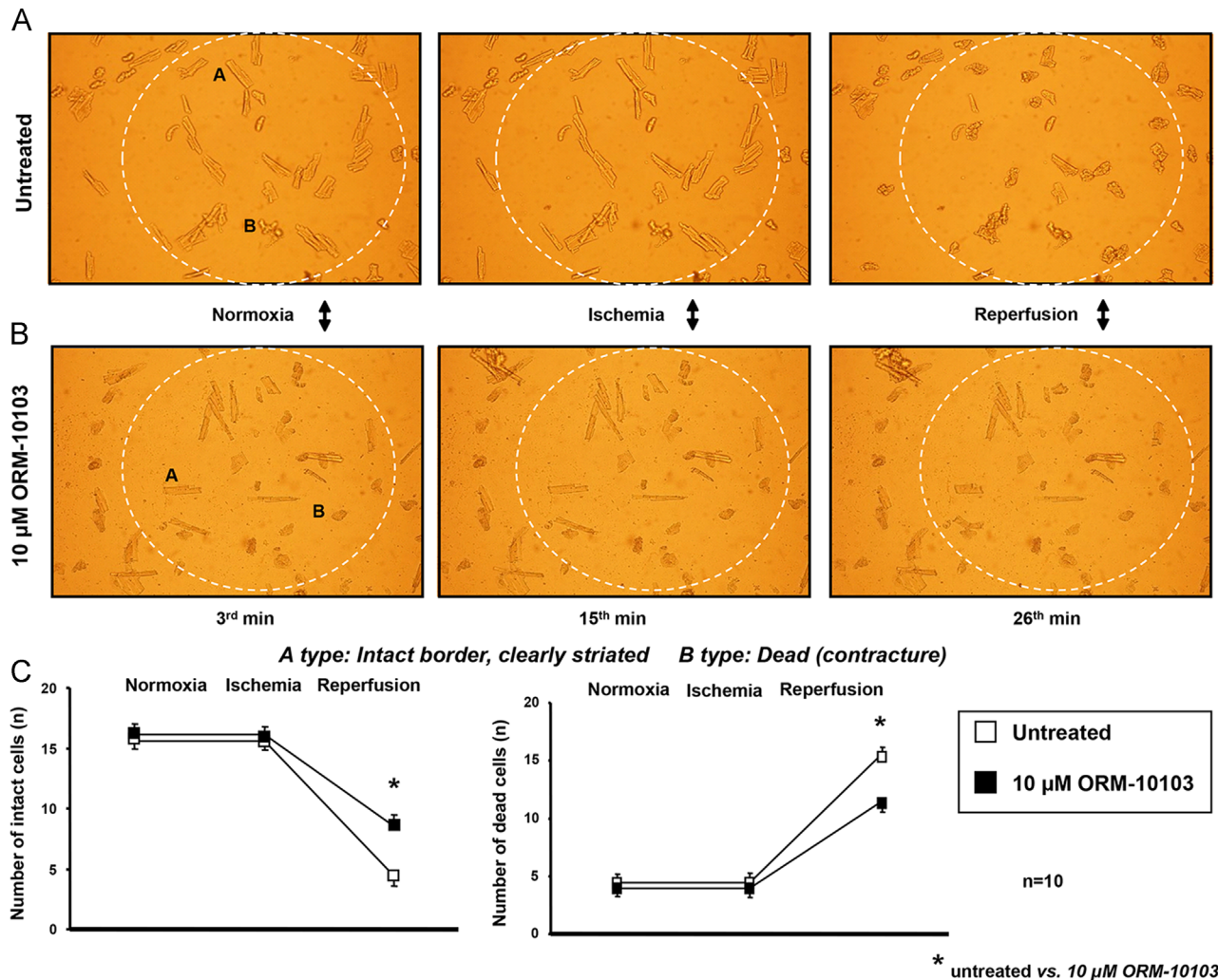
Fig. 1. Effect of 10 μM ORM-10103 on cardiomyocyte viability. (A, B) Representative selected microscope fields from a pair of experiments performed on untreated and ORM-10103 treated native cardiomyocytes. Still images were periodically captured using a digital photo camera. Classification of the cells was based on morphological variables: **Class A:** cells with normal, elongated shape, intact border and visible striation; **Class B:** cells dead or at the verge of death, in severe contracture, without apparent striation. (C) Mean values prior to (3rd min), during (15th min) and following (26th min) simulated ischemia. The asterisks indicate significant ($P < 0.05$) difference between individual untreated and ORM-10103 treated values.

at the end of the loading process their fluorescent dye content—even at identical $[Ca^{2+}]_i$—showed significant variations and this variability was fully reflected by the magnitude of the optical signals. Therefore, to avoid abnormally high standard deviations caused solely by the heterogeneity of the dye content, fluorescence values were normalized to the control period.

In contrast to the "survival" data shown in Fig. 1, all single cell data presented in Figs. 2–9 were obtained from *living* cardiomyocytes, surviving the ischemia/reperfusion protocol. Incomplete single cell measurements were discarded from data analysis. All values presented are arithmetic means $\pm$ S.E.M. All data were analyzed using Students t test for paired or unpaired data, as relevant. Differences were considered significant when P was less than 0.05.

3. Results

3.1. Effect of selective NCX inhibition on cardiomyocyte viability

The results obtained from the "survival" experiments are shown in Fig. 1. Representative microscope fields from a pair of experiments performed on untreated and ORM-10103 treated cardiomyocytes are shown in panels (A) and (B), respectively. For survival analysis

regions of interest (ROIs, white circles) containing $\sim$20 predominantly intact, contracting cardiomyocytes were selected at the beginning of the normoxic period (left panels). Based on their morphological characteristics cells in the ROI were classified into two groups: **Class A:** elongated cells with intact border and clearly visible striation. **Class B:** dead cells, or cells on the verge of death with no visible striation and typically in full contracture. At the end of the ischemic period most cardiomyocytes in both ROIs seem to be principally intact (mid panels). At the end of the reperfusion period, however, a substantial number of the cells was in contracture (right panels). This is especially true for the untreated group.

Mean values, determined for both groups in the last minute of the control (normoxic), ischemia and reperfusion periods, are shown in panel (C). The distribution of cells in the normoxic state was close to identical in both groups, and the majority of these cells was intact (78% and 81% in the untreated and ORM-10103 treated groups, respectively). As noted above, ischemia by itself apparently did not influence cell distribution in either group. In contrast, reperfusion had a detrimental effect on the untreated group: 71% (112 out of 156) of the cells intact at the end of ischemia died during reperfusion. Application of 10 μM ORM-10103 had a clearly protective effect on cell viability; significantly less, only 47% (76 out of 161) of the ORM-treated cells died by the end of the reperfusion period.
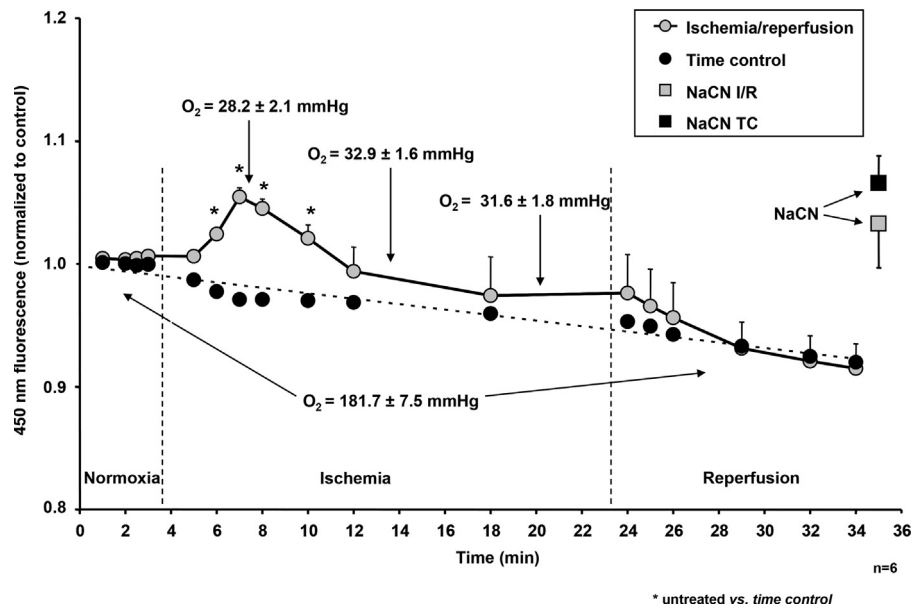
Fig. 2. Effect of simulated ischemia/reperfusion on NADH levels in isolated dye-free cardiomyocytes. In untreated, native cardiomyocytes NADH was excited at 360 nm, native fluorescence during the ischemia/reperfusion protocol has been monitored at 450 nm (gray circles). Nonspecific fluorescence shifts, caused by NADH bleaching, were estimated from normoxic (time control) cardiomyocytes (black circles). At the end of the protocols 10 mM sodium-cyanate (NaCN) was applied to induce maximal NADH reduction (squares). Asterisks indicate significant ($P < 0.05$) difference between individual ischemic and time control values ($n=6$).
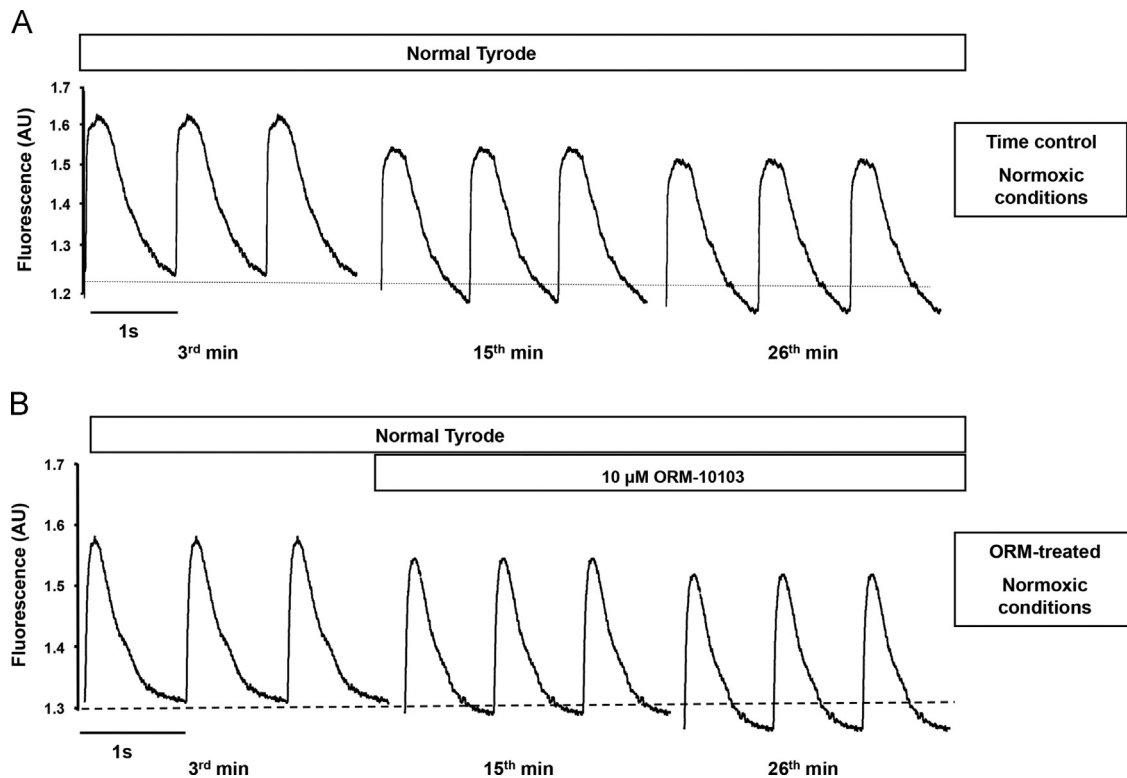

Fig. 3. Representative $[Ca^{2+}]_i$ transients recorded from untreated normoxic (time control) and ORM-10103 treated normoxic cardiomyocytes. In CaT measurements the cardiomyocytes were loaded with a Ca^{2+}-sensitive fluorescent dye, Fluo 4-AM. (A) Time control (normoxic) measurements were performed to enable the estimation of the rate of nonspecific fluorescence decay caused by dye leakage/extrusion. This decay factor was used to correct raw data obtained from all ischemia/reperfusion experiments. (B) In a predominant number of normoxic cardiomyocytes application of 10 μM ORM-10103 did not cause apparent changes in the magnitude, shape and decay kinetics of the transient, while in a minority of cells some decrease could be observed.

3.2. Validation of intracellular ischemia by monitoring NADH levels

The onset and relative depth of intracellular ischemia were verified by monitoring ischemia induced shifts in inherent fluorescence of dye-unloaded (native) cardiomyocytes and comparing those to nonspecific, time dependent fluorescence shifts developed in nonischemic cells. In order to estimate the depth of intracellular ischemia NaCN—a well known inhibitor of the mitochondrial cytaaa_3, often used to induce close to maximal short term reduction in NAD^+—was applied immediately following the reperfusion period. The results of the NADH fluorescence measurements are shown in Fig. 2.
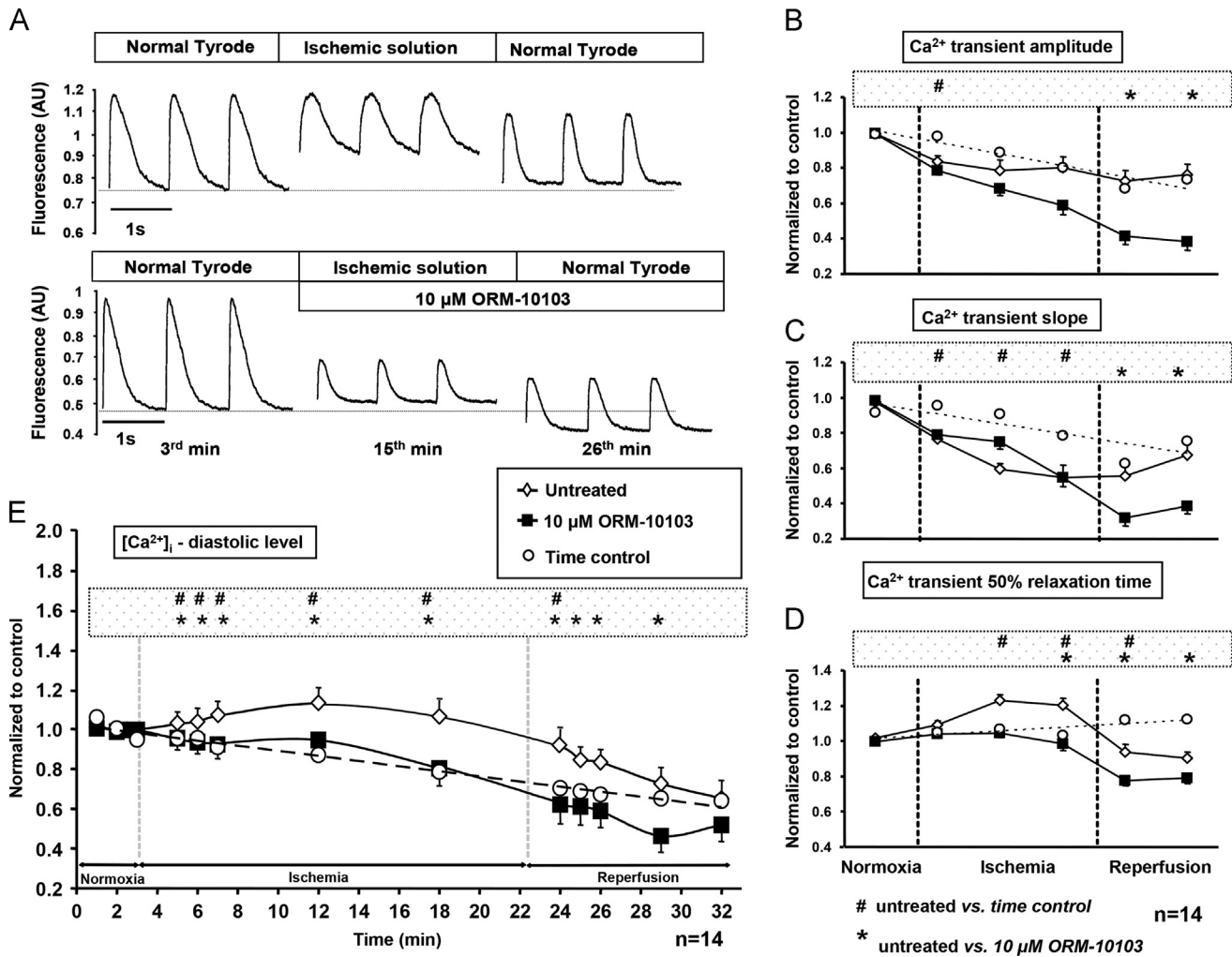
Fig. 4. Changes in major CaT parameters during simulated ischemia/reperfusion and the effect of 10 μM ORM-10103 treatment on these parameters in strophantidine-untreated cardiomyocytes. (A) Representative raw recordings of CaT from untreated (upper traces) and ORM-treated (lower traces) cells prior to, during and following simulated ischemia. CaTs shown in this panel were corrected for dye leakage and nonspecific background, but were not normalized. (B–E) Ischemia/reperfusion induced shifts in major CaT variables and the effect of 10 μM ORM-10103 on the (B) magnitude, (C) slope and (D) half-relaxation time of the transients. Parameter values were obtained in the 3rd min (control), 6th, 10th, and 15th min (early, mid and late phase of ischemia), and 26th and 30th min (early and late phase of reperfusion) of the recordings. (E) The changes in $[Ca^{2+}]_{iD}$ levels are shown in more details. Since the absolute level of the dye fluorescence depends on the size of the individual cells, as well, as their actual dye concentration, all experiments were self-controlled and all fluorescence values obtained during ischemia/reperfusion were normalized to the mean of the control values determined from the same cell for each minute during the normoxic period. (C) Slope values, calculated from the CaTs by fitting a line to the ON slope at its maximal increase rate (i.e. at the peak of the first derivative). Fluorescence data were analyzed using Students t test for paired or unpaired data, as relevant. Hash marks and asterisks indicate significant ($P < 0.05$) difference between individual time control vs. untreated and untreated vs. ORM-treated values, respectively. Since two of the three graphs depicted in these panels are often in close proximity, the commonly used placement of the significance marks (i.e. on top of the corresponding graphs) in these panels could be misleading. Therefore, both significance marks are shown in a separate bar on top of the panel.

In cells not exposed to ischemia (time control group) only a limited, gradual decrease in cellular fluorescence, most likely a consequence of nonspecific changes (bleaching), could be observed (black circles). In contrast, in cells exposed to the ischemia/reperfusion protocol cellular fluorescence increased significantly during the ischemic period (gray circles). When switching perfusion solutions ~30 s was necessary for the new perfusate to reach the chamber, and about further ~1 min to mix and decrease the oxygen level in the chamber low enough to induce anaerobic transition. Ischemia-induced NADH shifts were calculated by correcting raw fluorescence values for nonspecific changes (calculated from the time control measurements). Furthermore, all fluorescence data shown in Fig. 2 were normalized to the level obtained from the same cell at the beginning of the normoxic period.

In the early phase of ischemia a steep increase in [NADH] could be observed ($8.4 \pm 0.4\%$; $n=6$). During the ischemic cycle the level of the corrected fluorescence increase was varying, most probably

reflecting the minor variations in oxygen levels inside the chamber. During reperfusion [NADH] gradually returned to control level, even a minimal, insignificant undershoot could be observed. Compared to simulated ischemia, the application of cyanate induced significantly larger NAD^+ reduction (ischemic and time control cells: $12.2 \pm 2.8\%$ and $15.1 \pm 1.9\%$, respectively, $n=4$). During these measurements pO_2 levels were repetitively determined using a blood gas analyzer (ABL 505, Radiometer, Denmark) in 50 μl samples collected from the central area of the chamber. While the pO_2 level in the chamber was sufficiently high during normoxia (181.7 ± 7.5 mmHg, $n=25$) under ischemic perfusion it was always lower than 40 mmHg (32.9 ± 1.6 mmHg, $n=25$).

3.3. The effect of selective NCX inhibition on the $[Ca^{2+}]_i$ transient

A set of representative CaT waveforms is shown in Figs. 3–5. In time control measurements only a small, gradient decrease in the magnitude and baseline of the transient could be observed
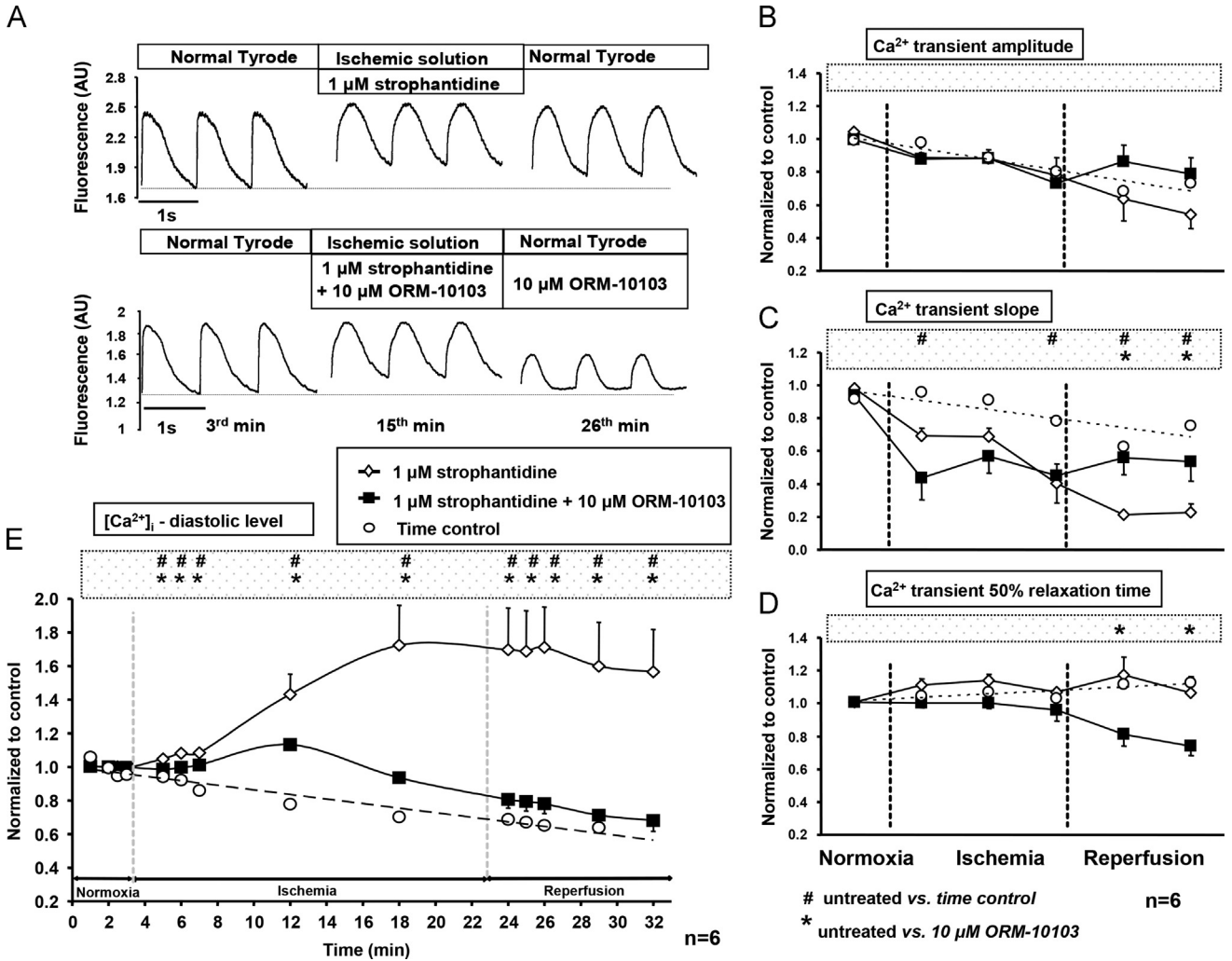
Fig. 5. Changes in major CaT parameters during simulated ischemia/reperfusion and the effect of 10 μM ORM-10103 treatment on these parameters in strophantidine-treated cardiomyocytes. (A) Representative raw recordings of CaT from untreated (upper traces) and ORM-treated (lower traces) cells prior to, during and following simulated ischemia. (B–E) Ischemia/reperfusion induced shifts in major CaT variables and the effect of 10 μM ORM-10103 on the (B) magnitude, (C) slope and (D) half-relaxation time of the transients, and (E) $[Ca^{2+}]_{iD}$ levels. All calculations and representations were performed as shown in Fig. 4.

(Fig. 3A). This gradual decrease is predominantly a consequence of dye leakage/extrusion from the cell. Interestingly, under normoxic conditions the application of 10 μM ORM-10103 had no apparent effect on the magnitude or kinetics of the transient (Fig. 3B). During simulated ischemia in both strophantidine untreated (Fig. 4A) and treated (Fig. 5A) cells significant changes in the magnitude and kinetics of the CaT could be observed. The traces shown in these panels were corrected for dye leakage (the rate of dye leakage/extrusion was approximated from time control recordings) and nonspecific background fluorescence (determined at the beginning and end of the recording, by removing the cell from the optical field), but— in contrast to all other (calculated) panels - were not normalized to the control traces. Compared to the normoxic waveforms (left traces), application of 10 μM ORM-10103 did not prevent or revert most of these changes (mid traces), indeed, it induced further alterations in both the magnitude and kinetics of the transient. During reperfusion neither groups could completely recover, whether untreated, or treated with 1 μM strophantidine or 10 μM ORM-10103 or both (right traces).

Ischemia/reperfusion induced changes in characteristic parameters of the CaT in *strophantidine-untreated* cells are shown in the panels B–E of Fig. 4. In this and a few other Figs. (Figs. 5 and 8) two distinct significance levels were calculated and presented: hashmarks (♯) and asterisks (∗) indicate significant difference

between *untreated vs. time control*, and *ORM-treated vs. untreated* values, respectively. Significant changes in the amplitude of the CaT in untreated compared to time control cells could only be observed during the early phase of ischemia (0.836 ± 0.03 vs. 0.979 ± 0.02; $n = 14$) (B). In contrast, 10 μM ORM-10103 caused a steady, gradual decrease in the amplitude of the CaT (0.76 ± 0.06 vs. 0.38 ± 0.05; $n = 14$), which became significant (compared to ORM-10103 untreated cells) during reperfusion. In the slope of the transient (C) ischemia induced a gradual, significant decrease in untreated cardiomyocytes compared to time control (0.55 ± 0.07 vs. 0.54 ± 0.05 $n = 14$) and ORM treatment had no apparent effect on this ecrease. On the other side, during reperfusion the slope in the two groups changed in opposite direction - recovered in untreated, further decreased in treated cells, the differences between the two groups became significant (0.67 ± 0.09 vs. 0.39 ± 0.04; $n = 14$). In untreated cells ischemia also caused a significant increase in the half-relaxation time (RT_{50}) of the CaT, compared to time control (D). In these cells RT_{50} recovered during reperfusion, typically with a moderate undershoot compared to time control. In contrast, treatment with ORM-10103 significant decreased RT_{50} (0.90 ± 0.03 vs. 0.79 ± 0.03; $n = 14$) during late ischemia and reperfusion, compared to untreated cells. The largest modulatory effect of ORM-10103 treatment could be observed in $[Ca^{2+}]_{iD}$ (E). As expected, ischemia induced a
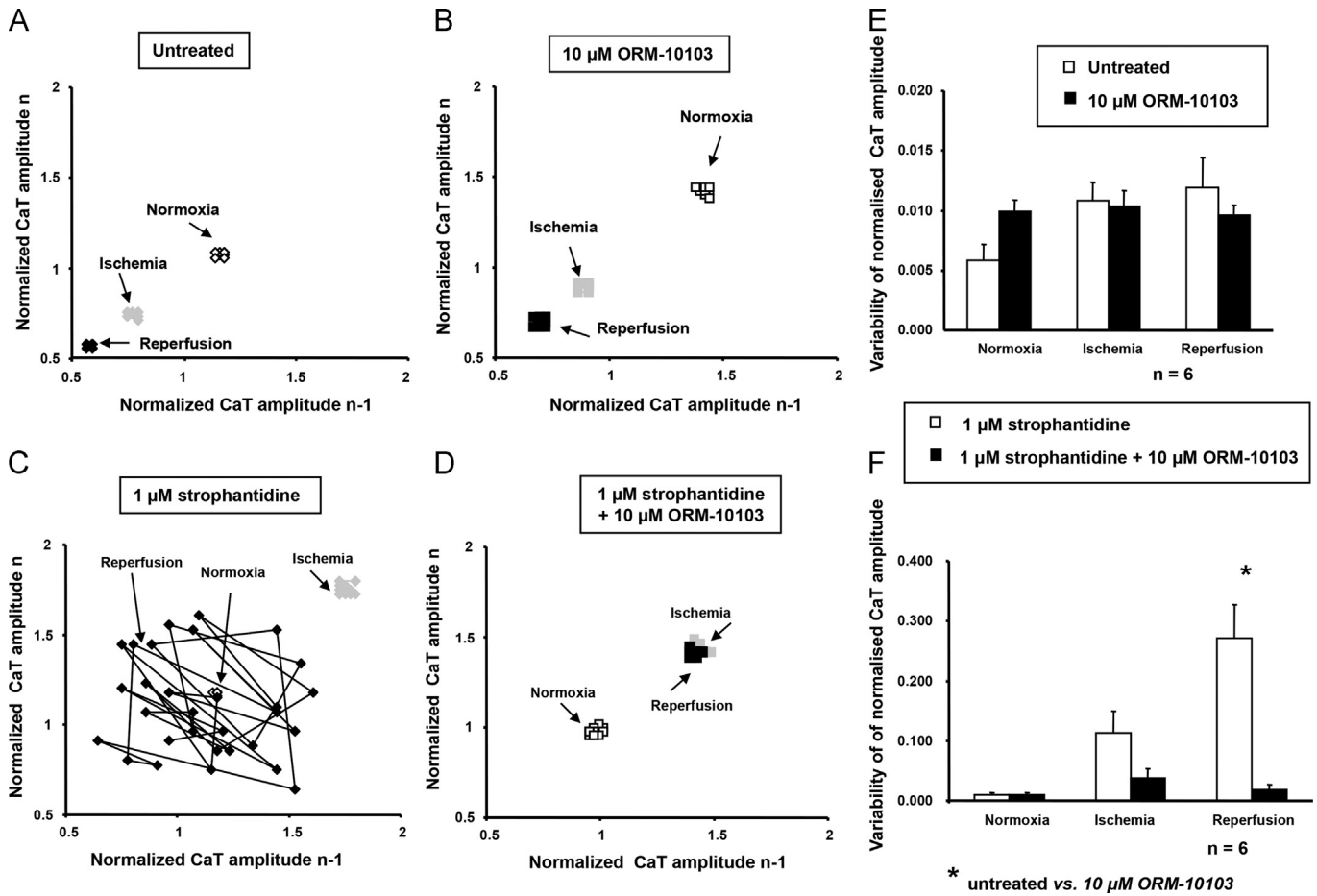
Fig. 6. The effect of 10 μM ORM-10103 on the amplitude variability of the $[Ca^{2+}]_i$ transient. Variabilities in the amplitude of the CaT were calculated from all four sets of experiments. Representative examples from untreated, ORM-treated, strophantidine-treated and strophantidine+ORM-treated are presented in panels (A), (B), (C) and (D), respectively. Summarized variabilities for the strophantidine-untreated and treated cardiomyocytes are shown in panels (E) and (F), respectively. The asterisk indicate significant ($P < 0.05$) difference between individual untreated and ORM-treated values.

substantial raise in $[Ca^{2+}]_{iD}$, which became significant by the 2nd min of ischemia. Upon reperfusion $[Ca^{2+}]_{iD}$ slowly normalized, however, during its early phase (~ 6 min) it was still significantly higher than in time control cells (1.04 ± 0.03 *vs.* 0.92 ± 0.02; $n=14$). Pretreatment of the cardiomyocytes with 10 μM ORM-10103 completely eliminated the raise in $[Ca^{2+}]_{iD}$ and by the end of the ischemic period it even decreased below time control (0.73 ± 0.08 *vs.* 0.64 ± 0.06; $n=14$). During reperfusion $[Ca^{2+}]_{iD}$ in these cells was permanently below control.

Ischemia/reperfusion induced changes in characteristic parameters of the CaT in *strophantidine treated* cells are shown in panels B–E of Fig. 5. In these cells no significant changes in the amplitude of the CaT could be observed during ischemia or reperfusion (B). Compared to time control, the slope of the CaT gradually, but significantly decreased during both ischemia and reperfusion (C). ORM-10103 failed to influence the ischemia induced fall in the slope of the CaT, but significantly limited its further decrease during reperfusion (0.55 ± 0.1 *vs.* 0.21 ± 0.02; $n=6$). In ORM-10103 untreated cells RT_{50} was close to the time control during both ischemia and reperfusion (D). In contrast, the application of 10 μM ORM-10103 induced a significant decrease in this parameter during reperfusion (1.17 ± 0.11 *vs.* 0.81 ± 0.06; $n=6$). The already significant ischemia-induced elevation in $[Ca^{2+}]_{iD}$, observed in the untreated myocytes, was further significantly augmented in strophantidine treated cells (E) and this marked increase was apparently maintained during the entire period of reperfusion. Application of 10 μM ORM-10103 completely eliminated the hugh ischemia induced elevation in $[Ca^{2+}]_{iD}$;

indeed, diastolic $[Ca^{2+}]_i$ levels in these cells did not differ significantly from levels measured in normoxic cardiomyocytes (0.71 ± 0.06 *vs.* 0.65 ± 0.06; $n=6$).

The beneficial effect of ORM-10103 treatment during reperfusion became even more evident by comparing short term variabilities of the CaT amplitudes. Variabilities calculated from all four experimental groups for the normoxic, ischemic and reperfusion periods are shown in Fig. 6. Representative Poincare plots, obtained in untreated, ORM-10103 treated, strophantidine treated and strophantidine+ORM-10103 treated cells, are shown in panels A, B, C and D, respectively. Mean data from untreated and ORM-10103 treated cells are provided in panel (E). As one can conclude from these diagrams, in untreated cells no apparent ischemia/reperfusion induced changes in CaT variabilities could be observed, while ORM 10103 treatment caused a small, rather insignificant decrease in both cases (0.011 ± 0.002 *vs.* 0.010 ± 0.001 and 0.012 ± 0.003 *vs.* 0.010 ± 0.001; $n=6$, during ischemia and reperfusion, respectively). In contrast, as shown in panel (F), during ischemia strophantidine significantly enhanced the short term variability (0.113 ± 0.037 *vs.* 0.037 ± 0.016; $n=6$) which was even further augmented during reperfusion (0.272 ± 0.055 *vs.* 0.018 ± 0.009; $n=6$). This large elevation was, again, fully eliminated by the application of 10 μM ORM-10103.

3.4. Effect of selective NCX inhibition on AP parameters

Representative AP waveforms are shown in Fig. 7. During normoxia 10 μM ORM-10103 evoked moderate APD shortening
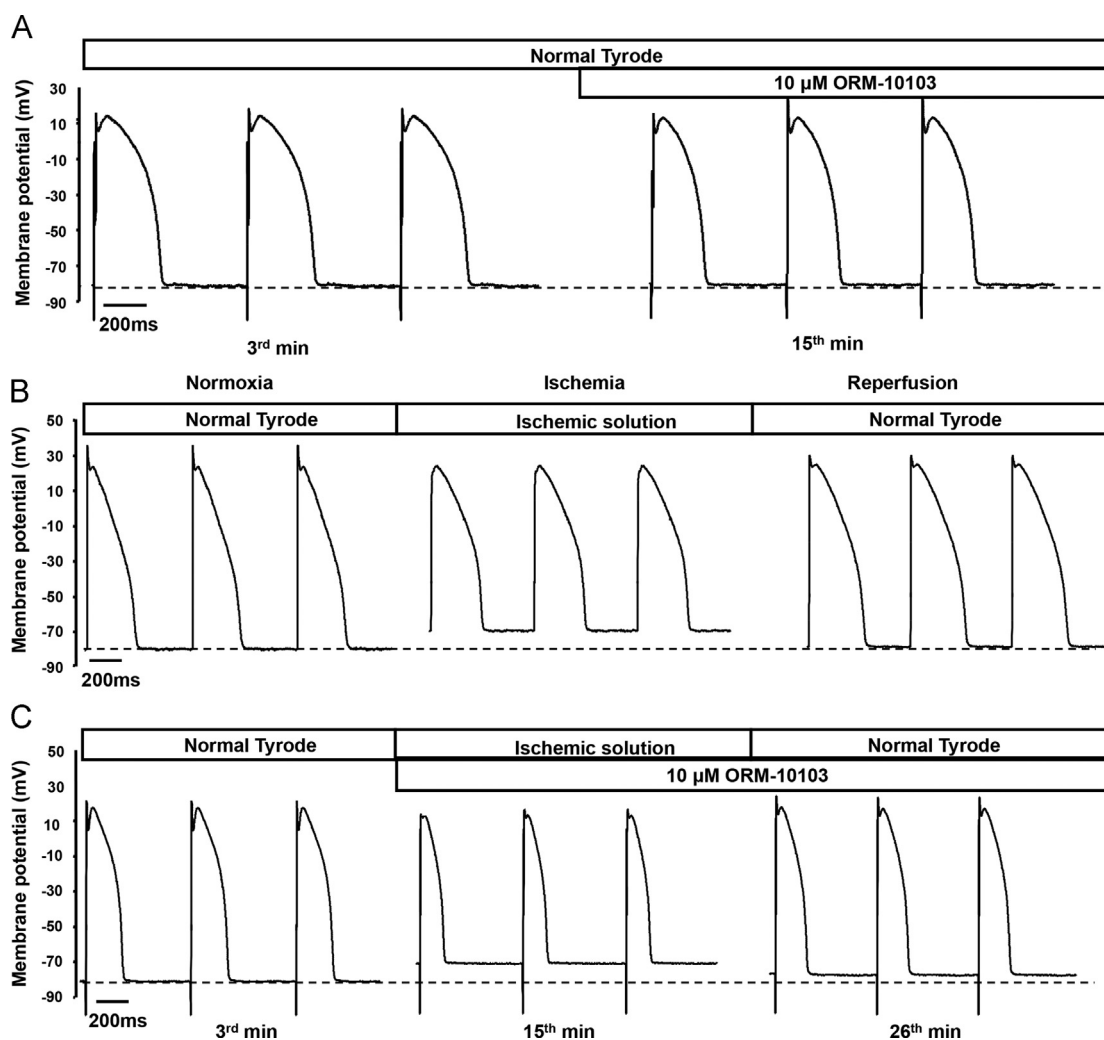
Fig. 7. Representative traces from the action potential measurements. AP measurements were performed in native (dye-unloaded) cells. (A) The effect of 10 μM ORM-10103 on normoxic cardiomyocytes. (B, C) The effect of the simulated ischemia/reperfusion protocol on action potentials recorded ORM-10103-untreated and treated cardiomyocytes, respectively.

without substantially modulating either its amplitude or the resting membrane potential (**A**). During simulated ischemia, however, significant changes in the shape and kinetics of the APs developed and the resting membrane potential was depolarized (middle trace in panel B). Both parameters were apparently normalized during reperfusion (right trace in panel B). The AP shortening effect of 10 μM ORM-10103 observed in normoxic cells was even more evident during both ischemia and reperfusion (panel C); however, no additional ORM-10103 induced shifts in AP could be observed. Indeed, the ORM-treatment failed to substantially reduce the ischemia induced depolarization of the resting membrane potential.

Ischemia/reperfusion induced alterations in the characteristic parameters of the AP in untreated and ORM-10103 treated cardiomyocytes are shown in Fig. 8. Compared to normoxic cells, ischemia induced a significant reduction in the amplitude, a substantial, but not significant decrease in the plateau level of the AP (A) and (B), and the resting membrane potential became significantly depolarized (C). These parameters were practically restored during reperfusion. ORM-10103 had no apparent effect on the magnitude of the ischemia induced shifts, neither on the recovery of these variables.

In order to characterize major changes in AP kinetics APD_{25} (D) and APD_{90} (E) were determined and from these variables AP triangulation was calculated (F). Ischemia induced a moderate

decrease in APD_{25} which was normalized during reperfusion. Compared to the untreated cells substantially larger decrease in APD_{25} could be observed in ORM-10103 treated cardiomyocytes, became significant in the late phase of ischemia and did not recover during reperfusion (0.90 ± 0.09 *vs.* 0.66 ± 0.09; $n=9$). Qualitatively similar, but augmented ischemia induced shortening could be observed in APD_{90}, however, the differences between the two groups were not significant during either ischemia or reperfusion. Compared to the time control cells, ischemia induced a large, significant decrease in AP triangulation in both groups, but again, the differences between the untreated and ORM-10103 treated groups were not significant (0.61 ± 0.07 *vs.* 0.76 ± 0.17; $n=9$).

The effect of ORM-10103 treatment during ischemia/reperfusion on the characteristics of the AP was further analyzed by calculating short term variabilities in APD_{90} and APD_{25}. Results of these calculations are shown in Fig. 9. Representative Poincare plots taken from untreated and ORM-10103 treated cardiomyocytes are presented in panels (A–D). The average values obtained in the APD_{90} and APD_{25} groups are shown in panels (E) and (F), respectively. Under normoxic conditions APD variabilities were similar in both groups. Ischemia induced moderate, but insignificant decrease in APD_{90} variabilities in the untreated group, while there was no apparent change in the ORM-10103 treated group. In contrast, APD_{25} variabilities failed to change in the control group, but showed a tendency to decrease following ORM-10103
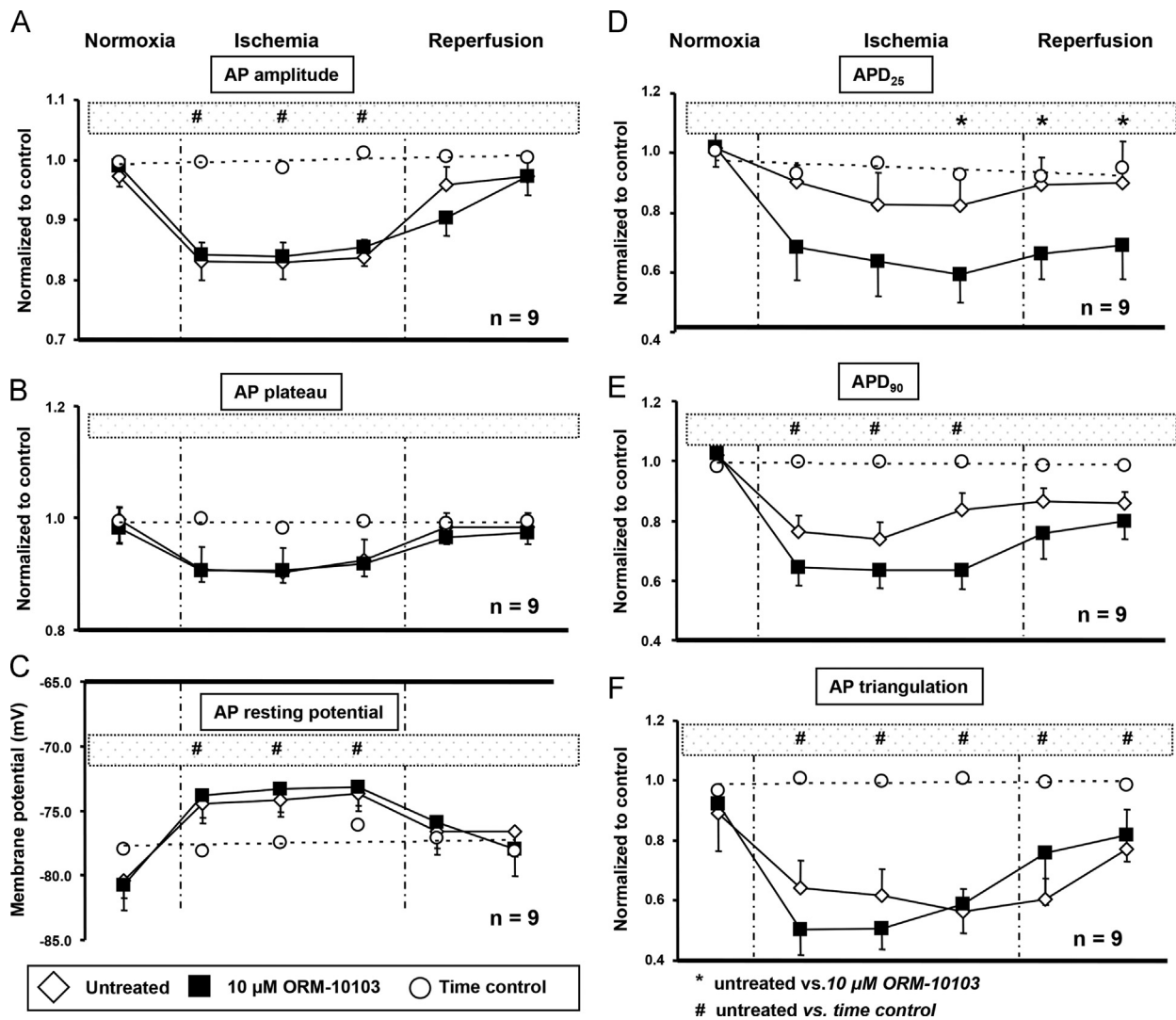
Fig. 8. Changes in major AP parameters during simulated ischemia/reperfusion and the effect of 10 μM ORM-10103 treatment on these parameters in strophantidine-untreated cardiomyocytes. (A) Amplitude; (B) plateau level; (C) resting membrane potential; (D) APD$_{25}$; (E) APD$_{90}$; and (F) triangulation. Parameter values were obtained in the 3rd min (control), 6th, 10th and 15th min (early, mid and late phase of ischemia), and 26th and 30th min (early and late phase of reperfusion) of the recordings. All data, except the resting membrane potential values, were normalized to the normoxic (control) period and analyzed using Students *t* test for paired or unpaired data, as relevant. Hash marks and asterisks indicate significant ($p < 0.05$) difference between individual time control *vs.* untreated and untreated *vs.* ORM-treated values, respectively. All significance marks are shown in a separate bar on top of the corresponding panel.

treatment. During reperfusion the only significant change was an elevation in APD$_{90}$ variabilities determined in the untreated group. ORM-10103 treatment eliminated this increase (5.37 ± 0.96 *vs.* 3.47 ± 0.69 ms; $n=9$).

4. Discussion

Since the Na$^+$/Ca^{2+} exchanger plays a crucial role in maintaining [Ca^{2+}]$_i$ homeostasis, any abnormal shift in its transport rate or direction exerts a significant impact on cardiac contractile function and electrical activity. Its augmented reverse mode transport induces [Ca^{2+}]$_i$ overload (e.g. during ischemia/reperfusion) and its increased forward mode activity leads to gradual [Ca^{2+}]$_i$ loss (e.g. in chronic heart failure) (Allen and Orchard, 1987; Diaz and Wilson, 2006; Frohlich et al., 2013). In both pathological conditions partial NCX inhibition may normalize the delicate balance in intracellular Ca^{2+} handling, resulting in effective protection against the progression of the disease. A number of previous studies provided important information on the consequences of NCX inhibition in healthy and diseased hearts (Inserte

et al., 2002; MacDonald and Howlett, 2008), however, correct interpretation of these results was seriously hampered by the lack of selectivity of the used inhibitors. Therefore, in the present study we evaluated the efficacy of a new, selective NCX inhibitor, ORM-10103 (Jost et al., 2013) to protect canine ventricular cardiomyocytes during simulated ischemia/reperfusion.

4.1. Cell viability

A most direct way to test the efficacy of the selective NCX blockade in protecting cardiomyocytes against ischemia/reperfusion injuries is to compare cell survival between untreated and treated groups (Fig. 1). Instead of using vital dyes, we followed a similarly effective classification, based simply on the shape and visibility of the striation of the cell (Maddaford et al., 1999). This form of classification may also have some benefits since with proper experience one is able to reliably dissect crippled, dying cardiomyocytes from safely surviving cells. The results of these experiments are straightforward and seem to support the hypothesis that partial, selective NCX inhibition by ORM-10103 may effectively protect the cardiomyocytes from severe ischemia/reperfusion
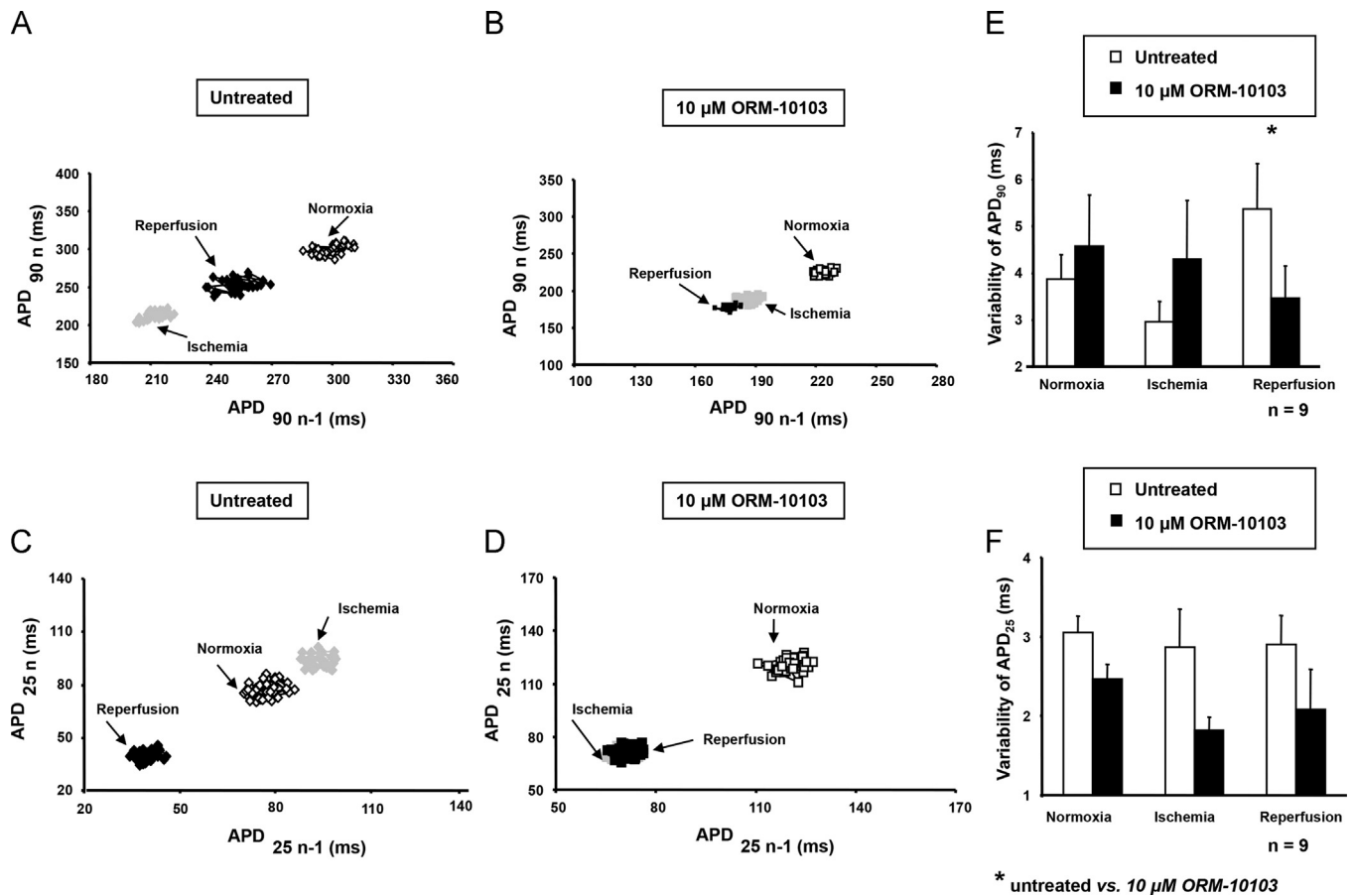
Fig. 9. The effect of 10 μM ORM-10103 on APD_{90} and APD_{25} variabilities. (A, B) and (C, D) Representative examples for calculated APD_{90} and APD_{25} variabilities determined from untreated and ORM-treated cardiomyocytes, respectively. (E) Summarized APD_{90} and (F) APD_{25} variabilities. The asterisk indicates significant ($P < 0.05$) difference between individual untreated and ORM-treated values.

induced injuries. This protection is most probably a direct consequence of the NCX inhibitory effect on the buildup of ischemia-induced Ca^{2+} overload leading to contracture and elevated $[Ca^{2+}]_{iD}$, which may severely compromise mitochondrial function (Eisner et al., 2005). A further contribution of ORM-10103 to cardiomyocyte survival may be its significant stabilizing effect on the CaT and APD by inhibiting the ischemic increase in their variabilities (Diaz et al., 2004).

4.2. Level of ischemia

During ischemia compromised oxidative metabolism leads to marked reduction in mitochondrial NAD^+ content, reflected in increased cellular fluorescence. Maximal short term raise in $[NADH]_m$ can be well approximated following cyanate application. The ratio of the magnitudes of fluorescence increase during ischemia and cyanate treatment is characteristic of the level of cellular ischemia. In this study the increase in cellular fluorescence during *simulated* ischemia was found to be substantially less than in the presence of cyanate (Fig. 2). Consequently, during this protocol oxidative metabolism was severely compromised, but not abolished (Lu et al., 2005). This is not surprising, since the oxygen level in the chamber was low, but not zero (32.9 ± 1.6 mmHg). Therefore, the simulated ischemia protocol is more suitable to model the lateral, low-flow zone than the central now-flow region of the infarcted area. As shown in Fig. 2 NADH fluorescence was above time control during the ischemic period and only returned to control level during reperfusion. The apparent gradual fluorescence decrease during the ischemic period was

probably not caused by bleaching only, since the rate of bleaching, estimated from the time control measurements, was substantially lower. Indeed, the bleaching-independent component of the decrease could originate from two principal sources. First, the pO_2 level, reached in the chamber, was probably very close to the critical pO_2 for isolated, active cardiomyocytes; consequently, even a small shift in chamber pO_2 could induce a marked shift in [NADH]. Another reason may be that in the absence of glucose the substrate availability during ischemia is decreasing, leading to partial reoxidation of the mitochondrial NADH pool. At this moment we have no specific data to settle this issue; both explanations are feasible and even may act simultaneously (Eng et al., 1989).

4.3. $[Ca^{2+}]_i$ transient

In the *ORM-untreated* cells all well known characteristic consequences of ischemia induced $[Ca^{2+}]_i$ accumulation could be observed (Fig. 3). Diastolic $[Ca^{2+}]_i$ rose (E) and since the amplitude of the CaT did not decrease simultaneously (B), systolic $[Ca^{2+}]_i$ increased, as well. The kinetic parameters CaT were also altered. The ON slope of the CaT was reduced (C); the half-relaxation time (RT_{50}) increased (D).

The background of these effects is highly complex: reduced SERCA activity following ATP depletion leads to decreased SR Ca^{2+} content (see the reduced slope and amplitude of the CaT); the depolarization in resting membrane potential decreases the *forward*, the high $[Na^+]_i$ increases the *reverse* activity of the NCX. The latter also facilitates Ca^{2+} influx, considerably increasing the

amount of $[Ca^{2+}]_i$ to be extruded (Bers, 2008; Lee and Allen, 1992). Reduced SERCA and forward NCX activities should lead to simultaneously decreased $[Ca^{2+}]_{SR}$ and elevated $[Ca^{2+}]_i$. Upon reperfusion the amplitude and slope of the CaT and (slowly) $[Ca^{2+}]_{iD}$ were restored (O'Brien et al., 2008). In contrast, RT_{50} was shortened. The acceleration of CaT relaxation during reperfusion may be related to the fast recovery of the $[K^+]_i$ and subsequent membrane repolarization, which, in turn, may significantly increase the efficacy of the forward NCX activity and facilitate the simultaneous recovery of the [ATP], subsequently normalizing SERCA activity. The reduction of RT_{50} below control level may reflect an "overshoot" in Ca^{2+} handling during recovery (Talukder et al., 2009).

Application of ORM-10103 had a significant impact on ischemia/reperfusion induced CaT alterations. The amplitude and slope of the CaT were gradually decreased, although these differences only became significant during reperfusion. The large decrease observed in the amplitude of the CaT may support the notion that during ischemia NCX mediated beat-to-beat Ca^{2+} influx has an important role in compensating reduced $[Ca^{2+}]_{SR}$. More importantly, the significant ischemia induced raise in $[Ca^{2+}]_{iD}$ and RT_{50} were fully blocked by ORM-10103. During reperfusion these parameters significantly further decreased, directly supporting the hypothesis that the predominant effect of NCX blockade during ischemia/reperfusion is an effective suppression of the Na_i^+-accumulation induced activation of the *reverse* mode NCX activity (Wei et al., 2007).

Further support of this conclusion was provided from the strophantidine experiments. By inhibition of the Na^+/K^+ ATP-ase strophantidine facilitates Na_i^+ accumulation and consequently, prolongs reverse NCX activity. Indeed, ischemia-induced $[Ca^{2+}]_{iD}$ raise was approximately doubled, and, in contrast to the untreated cells, even further increased during reperfusion. ORM-10103 effectively and completely blocked this raise (Fig. 4E).

Another, highly promising protective effect of ORM-10103 is shown in Fig. 5. In strophantidine-untreated cardiomyocytes the variability of CaT was limited, suggesting partially maintained feedback control of the Ca^{2+} release on transsarcolemmal Ca^{2+} fluxes. In these cells ORM-10103 had no significant effect on variability. In contrast, in strophantidine-treated cardiomyocytes CaT variabilities during ischemia and especially during reperfusion were substantially augmented, suggesting that the delicate balance between the trigger and the feed-back systems was severely disturbed, leading to large fluctuations in beat-to-beat Ca^{2+} release and substantial instability of the Ca-handling (Eisner et al., 2005). This raise was completely diminished by application of ORM-10103, whose effect may be contributed to the marked reduction in $[Ca^{2+}]_i$. Since elevated CaT variability is often considered as a sensitive cellular marker for increased arrhythmia propensity (Tokuno et al., 2000), a reasonable conclusion of these results is that ORM-10103 is likely to substantially decrease the incidence of ischemia/reperfusion induced triggered cardiac arrhythmias.

4.4. AP morphology

Ischemia/reperfusion induced arrhythmias are usually generated by two interdependent intracellular mechanisms: $[Ca^{2+}]_i$ overload and sarcolemma depolarization (MacDonald and Howlett, 2008). $[Ca^{2+}]_i$ overload induces increased leakage of the $[Ca^{2+}]_{SR}$, enhancing the probabilities of diastolic Ca^{2+} releases (Wei et al., 2007). The subsequent inward current (mainly via forward I_{NCX}) facilitates the onset of Ca^{2+}-dependent, potentially lethal ventricular arrhythmias (Nagy et al., 2004). During ischemia APD is significantly shortened. Membrane depolarization via elevated K_i^+ efflux reduces the activity of the Na^+ and Ca^{2+} channels and attenuates Ca^{2+} extrusion (Lukas and Antzelevitch,

1993). In contrast, augmented $[Ca^{2+}]_{iD}$ facilitates Ca^{2+} efflux via forward I_{NCX} activity. Finally, ATP depletion-activated $I_{K(ATP)}$ carries extra repolarizing current. The resulting redistribution of the Ca^{2+} and repolarizing K^+ fluxes may substantially contribute to increased short-term APD_{90} and CaT variabilities during reperfusion.

In normoxic cells ORM-10103 treatment induced moderate APD shortening (Fig. 6A) probably via inhibition of the forward I_{NCX}. Further changes in AP were not observed. During ischemia the sarcolemma depolarized (Fig. 6B) and the spike potential diminished, however, both parameters recovered during reperfusion. ORM-10103 treatment failed to protect the cardiomyocytes against ischemia-induced AP perturbations (Fig. 6C). The apparent failure of ORM-10103 to counteract ischemic AP changes is even more obvious in Fig. 7. The depressed AP amplitude (A) and plateau (B), increased triangulation (F) and substantial depolarization of the resting potential (C) were practically uninfluenced by ORM-10103 treatment. Indeed, the ischemia-induced APD shortening was even augmented (D) and (E). The reason for the inefficacy of ORM-10103 to prevent these arrhythmogenic disturbances in AP may be complex. Though $[Ca^{2+}]_i$ changes are important modulators of the AP (Louch et al., 2002), it is more dependent on the balance of the inward Na^+, Ca^{2+} and outward K^+ currents. Except for a minimal decrease in the fast component of the delayed rectifier potassium current (I_{Kr}) neither of these factors are affected by ORM-10103 (Jost et al., 2013). This may be the primary cause for the minimal sensitivity of the AP to selective NCX blockade.

The only apparent beneficial effect of ORM-10103 on variables of the action potential was a significant reduction in reperfusion-induced raise of APD_{90} variabilities (Fig. 8). This may be a consequence of the increased stability of Ca^{2+}-handling and is most probably a consequence of the decreased $[Ca^{2+}]_i$ overload and reduced $[Ca^{2+}]_{iD}$ (Wei et al., 2007).

4.5. Limitations

It must be emphasized, that the data shown in Fig. 1 principally differ from data presented in Figs. 2–9. "Survival" experiments were performed on full cell populations (the only criterion when selecting the ROI at the beginning of the experiments was to find an area with predominantly healthy, contracting cells). Our present data shown in Fig. 1 and data in the literature (Moens et al., 2005) clearly demonstrate that a significant fraction of the cardiomyocytes does not survive the simulated ischemia protocol and dies during the reperfusion period. Since incomplete measurements were discarded from further proccessing, all single cell (NADH, CaT, AP) data presented were obtained from a limited cellular pool – i.e. surviving cells.

5. Conclusion

A major conclusion of the present study is that ORM-10103 treatment proved to be highly effective against ischemia/reperfusion induced arrhythmogenic shifts in $[Ca^{2+}]_i$ homeostasis by limiting the $[Ca^{2+}]_i$ overload and eliminating the ischemia-induced raise in diastolic $[Ca^{2+}]_i$. This beneficial effect may primarily be contributed to the inhibition of the significantly enhanced reverse mode activity of the Na^+/Ca^{2+} exchanger, activated by the increased $[Na^+]_i$. Furthermore, ORM-10103 seems to restore the markedly weakened reperfusion-induced stability of the $[Ca^{2+}]_i$ transient and significantly facilitates the post-reperfusion survival of the cardiomyocytes. However, in certain pathological conditions the efficacy of its protective effect may be hampered by its apparent inability to protect the heart against the arrhythmogenic disturbances in AP morphology.

References

Acsai, K., Kun, A., Farkas, A.S., Fulop, F., Nagy, N., Balazs, M., Szentandrassy, N., Nanasi, P.P., Papp, J.G., Varro, A., Toth, A., 2007. Effect of partial blockade of the $Na^{(+)}/Ca^{(2+)}$-exchanger on $Ca^{(2+)}$ handling in isolated rat ventricular myocytes. Eur. J. Pharmacol. 576, 1–6.

Allen, D.G., Orchard, C.H., 1987. Myocardial contractile function during ischemia and hypoxia. Circ. Res. 60, 153–168.

Anderson, S., 2002. Response to: effect of inhibition of Na^+/Ca^+ exchanger at the time of myocardial reperfusion on hypercontracture and cell death. Cardiovasc. Res. 55, 706–707.

Baczko, I., Giles, W.R., Light, P.E., 2003. Resting membrane potential regulates $Na^{(+)}$-Ca^{2+} exchange-mediated Ca^{2+} overload during hypoxia-reoxygenation in rat ventricular myocytes. J. Physiol. 550, 889–898.

Bers, D.M., 2008. Calcium cycling and signaling in cardiac myocytes. Annu. Rev. Physiol. 70, 23–49.

Birinyi, P., Acsai, K., Banyasz, T., Toth, A., Horvath, B., Virag, L., Szentandrassy, N., Magyar, J., Varro, A., Fulop, F., Nanasi, P.P., 2005. Effects of SEA0400 and KB-R7943 on Na^+/Ca^{2+} exchange current and L-type Ca^{2+} current in canine ventricular cardiomyocytes. Naunyn Schmiedebergs Arch. Pharmacol. 372, 63–70.

Bourdillon, P.D., Poole-Wilson, P.A., 1981. Effects of ischaemia and reperfusion on calcium exchange and mechanical function in isolated rabbit myocardium. Cardiovasc. Res. 15, 121–130.

Diaz, M.E., O'Neill, S.C., Eisner, D.A., 2004. Sarcoplasmic reticulum calcium content fluctuation is the key to cardiac alternans. Circ. Res. 94, 650–656.

Diaz, M.E., Trafford, A.W., O'Neill, S.C., Eisner, D.A., 1997. Measurement of sarcoplasmic reticulum Ca^{2+} content and sarcolemmal Ca^{2+} fluxes in isolated rat ventricular myocytes during spontaneous Ca^{2+} release. J. Physiol. 501, 3–16.

Diaz, R.J., Wilson, G.J., 2006. Studying ischemic preconditioning in isolated cardiomyocyte models. Cardiovasc. Res. 70, 286–296.

Eisner, D.A., Diaz, M.E., Li, Y., O'Neill, S.C., Trafford, A.W., 2005. Stability and instability of regulation of intracellular calcium. Exp. Physiol. 90, 3–12.

Eng, J., Lynch, R.M., Balaban, R.S., 1989. Nicotinamide adenine dinucleotide fluorescence spectroscopy and imaging of isolated cardiac myocytes. Biophys. J. 55, 621–630.

Frohlich, G.M., Meier, P., White, S.K., Yellon, D.M., Hausenloy, D.J., 2013. Myocardial reperfusion injury: looking beyond primary PCI. Eur. Heart J. 34, 1714–1722.

Haigney, M.C., Miyata, H., Lakatta, E.G., Stern, M.D., Silverman, H.S., 1992. Dependence of hypoxic cellular calcium loading on $Na^{(+)}$–Ca^{2+} exchange. Circ. Res. 71, 547–557.

Inserte, J., Garcia-Dorado, D., Ruiz-Meana, M., Padilla, F., Barrabes, J.A., Pina, P., Agullo, L., Piper, H.M., Soler-Soler, J., 2002. Effect of inhibition of $Na^{(+)}/Ca^{(2+)}$ exchanger at the time of myocardial reperfusion on hypercontracture and cell death. Cardiovasc. Res. 55, 739–748.

Jost, N., Nagy, N., Corici, C., Kohajda, Z., Horvath, A., Acsai, K., Biliczki, P., Levijoki, J., Pollesello, P., Koskelainen, T., Otsomaa, L., Toth, A., Papp, J.G., Varro, A., Virag, L., 2013. ORM-10103, a novel specific inhibitor of the Na^+/Ca^{2+} exchanger, decreases early and delayed afterdepolarizations in the canine heart. Br. J. Pharmacol. 170, 768–778.

Ladilov, Y., Haffner, S., Balser-Schafer, C., Maxeiner, H., Piper, H.M., 1999. Cardioprotective effects of KB-R7943: a novel inhibitor of the reverse mode of Na^+/Ca^{2+} exchanger. Am. J. Physiol. 276, H1868–H1876.

Lee, J.A., Allen, D.G., 1992. Changes in intracellular free calcium concentration during long exposures to simulated ischemia in isolated mammalian ventricular muscle. Circ. Res. 71, 58–69.

Louch, W.E., Ferrier, G.R., Howlett, S.E., 2002. Changes in excitation-contraction coupling in an isolated ventricular myocyte model of cardiac stunning. Am. J. Physiol. Heart Circ. Physiol. 283, H800–H810.

Lu, J., Zang, W.J., Yu, X.J., Chen, L.N., Zhang, C.H., Jia, B., 2005. Effects of ischaemia-mimetic factors on isolated rat ventricular myocytes. Exp. Physiol. 90, 497–505.

Lukas, A., Antzelevitch, C., 1993. Differences in the electrophysiological response of canine ventricular epicardium and endocardium to ischemia. Role of the transient outward current. Circulation 88, 2903–2915.

MacDonald, A.C., Howlett, S.E., 2008. Differential effects of the sodium calcium exchange inhibitor, KB-R7943, on ischemia and reperfusion injury in isolated guinea pig ventricular myocytes. Eur. J. Pharmacol. 580, 214–223.

Maddaford, T.G., Hurtado, C., Sobrattee, S., Czubryt, M.P., Pierce, G.N., 1999. A model of low-flow ischemia and reperfusion in single, beating adult cardiomyocytes. Am. J. Physiol. 277, H788–H798.

Moens, A.L., Claeys, M.J., Timmermans, J.P., Vrints, C.J., 2005. Myocardial ischemia/reperfusion-injury, a clinical view on a complex pathophysiological process. Int. J. Cardiol. 100, 179–190.

Nagy, Z.A., Virag, L., Toth, A., Biliczki, P., Acsai, K., Banyasz, T., Nanasi, P., Papp, J.G., Varro, A., 2004. Selective inhibition of sodium-calcium exchanger by SEA-0400 decreases early and delayed after depolarization in canine heart. Br. J. Pharmacol. 143, 827–831.

O'Brien, J.D., Ferguson, J.H., Howlett, S.E., 2008. Effects of ischemia and reperfusion on isolated ventricular myocytes from young adult and aged Fischer 344 rat hearts. Am. J. Physiol. Heart Circ. Physiol. 294, H2174–H2183.

Schafer, C., Ladilov, Y., Inserte, J., Schafer, M., Haffner, S., Garcia-Dorado, D., Piper, H. M., 2001. Role of the reverse mode of the Na^+/Ca^{2+} exchanger in reoxygenation-induced cardiomyocyte injury. Cardiovasc. Res. 51, 241–250.

Takahashi, K., Takahashi, T., Suzuki, T., Onishi, M., Tanaka, Y., Hamano-Takahashi, A., Ota, T., Kameo, K., Matsuda, T., Baba, A., 2003. Protective effects of SEA0400, a novel and selective inhibitor of the Na^+/Ca^{2+} exchanger, on myocardial ischemia-reperfusion injuries. Eur. J. Pharmacol. 458, 155–162.

Talukder, M.A., Zweier, J.L., Periasamy, M., 2009. Targeting calcium transport in ischaemic heart disease. Cardiovasc. Res. 84, 345–352.

Tanaka, H., Nishimaru, K., Aikawa, T., Hirayama, W., Tanaka, Y., Shigenobu, K., 2002. Effect of SEA0400, a novel inhibitor of sodium-calcium exchanger, on myocardial ionic currents. Br. J. Pharmacol. 135, 1096–1100.

Tokuno, T., Muraki, K., Watanabe, M., Imaizumi, Y., 2000. Protective effect of benidipine against the abnormal electrical activity in single ventricular myocytes of the guinea pig under simulated ischemic conditions and reperfusion. Jpn. J. Pharmacol. 82, 199–209.

Volders, P.G., Vos, M.A., Szabo, B., Sipido, K.R., de Groot, S.H., Gorgels, A.P., Wellens, H.J., Lazzara, R., 2000. Progress in the understanding of cardiac early afterdepolarizations and torsades de pointes: time to revise current concepts. Cardiovasc. Res. 46, 376–392.

Wang, J., Zhang, Z., Hu, Y., Hou, X., Cui, Q., Zang, Y., Wang, C., 2007. SEA0400, a novel Na^+/Ca^{2+} exchanger inhibitor, reduces calcium overload induced by ischemia and reperfusion in mouse ventricular myocytes. Physiol. Res. 56, 17–23.

Wei, G.Z., Zhou, J.J., Wang, B., Wu, F., Bi, H., Wang, Y.M., Yi, D.H., Yu, S.Q., Pei, J.M., 2007. Diastolic Ca^{2+} overload caused by Na^+/Ca^{2+} exchanger during the first minutes of reperfusion results in continued myocardial stunning. Eur. J. Pharmacol. 572, 1–11.

Zucchi, R., Ronca-Testoni, S., 1997. The sarcoplasmic reticulum Ca^{2+} channel/ryanodine receptor: modulation by endogenous effectors, drugs and disease states. Pharmacol. Rev. 49, 1–51.